Research Journal of Applied Sciences, Engineering and Technology 4(7): 754-763, 2012
ISSN: 2040-7467

Submitted: September 29, 2011 Accepted: October 23, 2011 Published: April 01, 2012

STATCOM Control for Operation under System Uncertainties

Shoorangiz Shams Shamsabad Farahani, Mehdi Nikzad, Mohammad Bigdeli Tabar, Hossein Tourang and Behrang Yousefpour
Department of Electrical Engineering, Islamshahr Branch, Islamic Azad University, Tehran, Iran

Abstract: In this study a robust controller is proposed to provide a robust performance under system uncertainties through static compensator (STATCOM) devices. The method of multiplicative uncertainty has been employed to model the variations of the operating conditions in the system. A Quantitative Feedback Theory (QFT) method based on loop shaping is employed to select a suitable open-loop transfer function. The design is carried out by applying robustness criteria for stability and performance. In order to show the effectiveness of our proposed controllers, the proposed controllers have been compared with classical controllers. The robust controller design has been demonstrated to provide extremely good dynamic performance over a range of operating conditions.

Key words: Flexible AC transmission systems, robust control, static compensator, system uncertainties

INTRODUCTION

Static var compensation can be utilized to regulate voltage, control power factor, and stabilize power flow (Hingorani *et al*., 2000). Most var compensators employ a combination of fixed or switched capacitance and thyristor controlled reactance. Static var compensators based on a voltage sourced inverter are known as STATCOMs. Considerable efforts have been done to further improve performance, decrease size, and increase flexibility of STATCOMs in (Edwards *et al*., 1988; Mori *et al*., 1993; Schauder *et al*., 1994).The basic principle about operation of a STATCOM is the generation of a controllable AC voltage source behind a transformer leakage reactance by a voltage source converter connected to a DC capacitor. The voltage difference across the reactance produces active and reactive power exchanges between the STATCOM and the power system (Wang and Li, 2000b). Two basic controls are implemented in a STATCOM. The first is the AC voltage regulation of the power system, which is realized by controlling the reactive power interchange between the STATCOM and the power system. The other is the control of the DC voltage across the capacitor through which the active power injection from the STATCOM to the power system is controlled (Wang and Li, 2000a, b). The effect of stabilizing controls on STATCOM controllers has been also investigated in several recent reports (Wang and Li, 2000a, b). PI controllers have been found to provide stabilizing controls when the AC and DC regulators were designed independently, However, the joint operations of them have been reported to lead to system instability because of the interaction of the two controllers (Wang and Li, 2000b; Wang, 1999a). While superimposing the damping controller on the AC regulator can circumvent the negative interaction problem, the fixed parameter PI controllers have been found invalid, as they lead to negative damping for certain system parameters and loading conditions (Li *et al*., 1998). Application of control methods performing over a range of operating conditions has also been reported in recent times. In (Farasangi *et al.,* 2000) a robust controller for SVC and STATCOM devices using H_∞ techniques has been proposed. Robust control for FACTS devices and their interaction with loads were examined in (Ammari *et al*., 2000). These designs are often complicated, restricting their realization.

The objective of this study is to investigate STATCOM control problem for a Single-Machine Infinite-Bus (SMIB) power system installed with a STATCOM. The variations of the operating conditions in the power system have been taken into consideration by modeling them as multiplicative unstructured uncertainty. There are two general design methodologies to deal with the effects of uncertainty:

- Adaptive control, in which the parameters of the plant are identified online and the obtained information is then used to tune the controller
- Robust control, which typically involves a worst-case design approach for a family of plants (representing the uncertainty) using a single fixed controller

In this study Quantitative Feedback Theory (QFT) is applied to design STATCOM controllers to systematically

Corresponding Author: Shoorangiz Shams Shamsabad Farahani, Department of Electrical Engineering, Islamshahr Branch, Islamic Azad University, Tehran, Iran

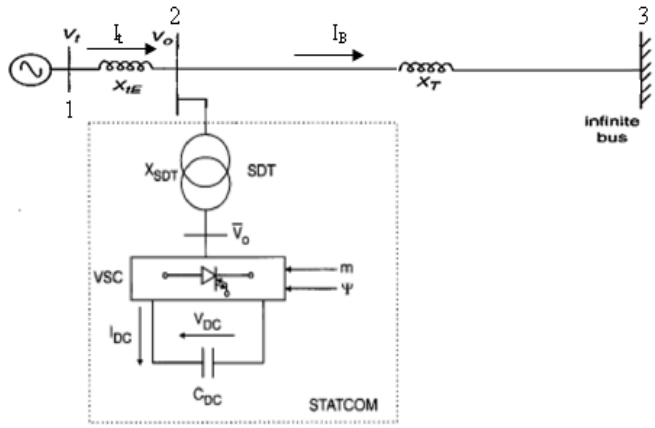

Fig. 1: A single-machine infinite-bus power system installed with STATCOM

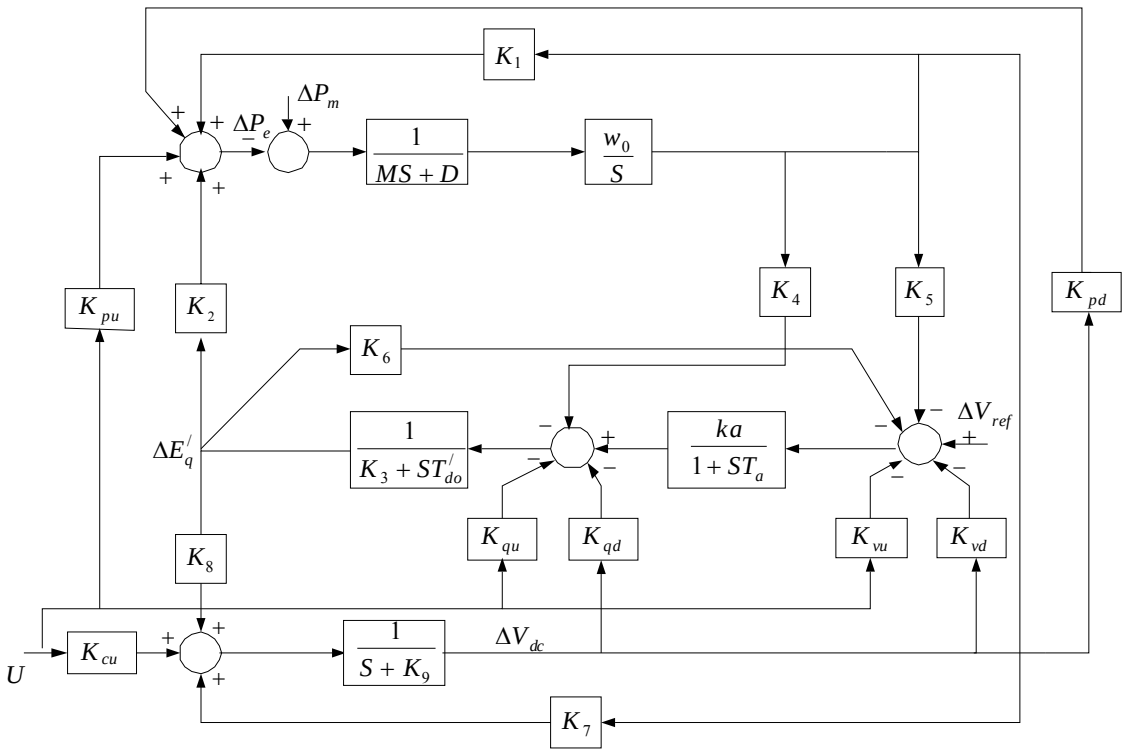

Fig. 2: Transfer function model of the system including STATCOM

deal with the effects of uncertainty. The proposed method has been successfully applied to design SISO and MIMO systems, nonlinear and time-varying cases (Dazzo and Houpis, 1988; Horowitz, 1982; Horowitz, 1979; Taher *et al*., 2009; Taher *et al*., 2008b, c). To show the effectiveness of robust control method, the proposed method is compared with classical method. Simulations Results show that the robust controllers guarantee robust performance under a wide range of operating conditions.

METHODOLOGY

System under study: A Single Machine Infinite Bus power system with a STATCOM connected through a step-down transformer is shown in Fig. 1 (Hingorani, 2000). The static excitation system, model type IEEE-ST1A, has been considered. It is assumed that the STATCOM is based on Pulse Width Modulation (PWM) converters. The nominal system parameters are given in Appendix.

Dynamic model of the system:

Non-linear dynamic model: A non-linear dynamic model of the system is derived by disregarding the resistances of all the system components (generator, transformers and transmission lines) and the transients of the transmission lines and transformer (Wang, 1999b). The nonlinear dynamic model of the system is given as (1).

$$\begin{cases} \dot{\omega} = (P_m - P_e - D\omega)/M \\ \dot{\delta} = \omega_0(\omega - 1) \\ \dot{E}' = (-E_q + E_{fd})/T'_{do} \\ \dot{E}_{fd} = (-E_{fd} + K_a(V_{ref} - V_t))/T_a \\ \dot{V}_{dc} = \dfrac{3m_E}{4C_{dc}}(\sin(\delta_E)I_{Ed} + \cos(\delta_E)I_{Eq}) \end{cases} \quad (1)$$

Linear dynamic model: A linear dynamic model is obtained by linearizing the non-linear dynamic model around the nominal operating condition. The linearized model is given as (2):

$$\begin{cases} \Delta\dot{\delta} = \omega_0 \Delta\omega \\ \Delta\dot{\omega} = (-\Delta P_e - D\Delta\omega)/M \\ \Delta\dot{E}'_q = (-\Delta E_q + \Delta E_{fd})/T'_{do} \\ \Delta\dot{E}_{fd} = -(1/T_A)\Delta E_{fd} - (K_A/T_A)\Delta V_t \\ \Delta\dot{v}_{dc} = K_7\Delta\delta + K_8\Delta E'_q - K_9\Delta v_{dc} + K_{ce}\Delta m_E \\ + K_{c\delta E}\Delta\delta_E \end{cases} \quad (2)$$

In (2), the parameters are defined as follow:

$$\Delta P_e = K_1\,\Delta\delta + K_2\,\Delta E'_q + K_{pd}\,\Delta v_{dc} + K_{pe}\,\Delta m_E + K_{p\delta E}\,\Delta\delta_E$$
$$\Delta E_q = K_3\,\Delta\delta + K_4\,\Delta E'_q + K_{qd}\,\Delta v_{dc} + K_{qe}\,\Delta m_E + K_{q\delta E}\,\Delta\delta_E$$
$$\Delta V_t = K_5\,\Delta\delta + K_6\,\Delta E'_q + K_{vd}\,\Delta v_{dc} + K_{ve}\,\Delta m_E + K_{v\delta E}\,\Delta\delta_E$$

Figure 2 shows the transfer function model of the system including STATCOM. The model has 20 constants denoted by K_{ij}. These constants are function of system parameters and the initial operating condition. The control vector U in Fig. 2 is defined as (3):

$$U = [\Delta m_E \quad \Delta\delta_E]^T \quad (3)$$

where,

Dm_E : Deviation in pulse width modulation index m_E of shunt inverter. By controlling m_E, the output voltage of the shunt converter is controlled

$\Delta\delta_E$: Deviation in phase angle of the shunt inverter voltage

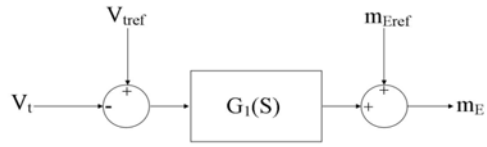

Fig. 3: AC-voltage regulator

It may be noted that in Fig. 2 K_{pu}, K_{qu}, K_{vu} and K_{cu} are row vectors and defined as below:

$$K_{pu} = [\,K_{pe} \quad K_{p\delta E}];\ K_{qu} = [K_{qe} \quad K_{q\delta E}]$$
$$K_{vu} = [K_{ve} \quad K_{v\delta E}];\ K_{cu} = [\,K_{ce} \quad K_{c\delta E}]$$

Dynamic model in state-space form: The dynamic model of the system in the state-space form is obtained as (4):

$$\begin{bmatrix} \Delta\dot{\delta} \\ \Delta\dot{\omega} \\ \Delta\dot{E}'_q \\ \Delta\dot{E}_{fd} \\ \Delta\dot{V}_{dc} \end{bmatrix} = \begin{bmatrix} 0 & \omega_0 & 0 & 0 & 0 \\ -\dfrac{K_1}{M} & 0 & -\dfrac{K_2}{M} & 0 & -\dfrac{K_{pd}}{M} \\ -\dfrac{K_4}{T'_{do}} & 0 & -\dfrac{K_3}{T'_{do}} & -\dfrac{1}{T'_{do}} & -\dfrac{K_{qd}}{T'_{do}} \\ -\dfrac{K_A K_5}{T_A} & 0 & -\dfrac{K_A K_6}{T_A} & -\dfrac{1}{T_A} & -\dfrac{K_A K_{vd}}{T_A} \\ K_7 & 0 & K_8 & 0 & -K_9 \end{bmatrix} \times \begin{bmatrix} \Delta\delta \\ \Delta\omega \\ \Delta E'_q \\ \Delta E_{fd} \\ \Delta V_{dc} \end{bmatrix} + \begin{bmatrix} 0 & 0 \\ -\dfrac{K_{pe}}{M} & -\dfrac{K_{p\delta E}}{M} \\ -\dfrac{K_{qe}}{T'_{do}} & -\dfrac{K_{q\delta E}}{T'_{do}} \\ -\dfrac{K_A K_{vc}}{T_A} & -\dfrac{K_A K_{v\delta E}}{T_A} \\ K_{ce} & K_{c\delta E} \end{bmatrix} \times \begin{bmatrix} \Delta m_E \\ \Delta\delta_E \end{bmatrix} \quad (4)$$

The typical values of the system parameters for the nominal operating condition are given in Appendix. The system parametric uncertainties are obtained 40% load change from their normal values in case of active and reactive power. Based on these uncertainties, six operating conditions are defined and shown in Appendix.

STATCOM control strategy: STATCOM control strategy comprises three controllers as follows:

- AC-voltage regulator (generator terminals voltage regulator)
- DC-voltage regulator
- Power system oscillations-damping controller

AC-voltage and DC-voltage regulators: AC-voltage regulator controls the generator terminal voltage which is regulated by modulating the magnitude of the shunt converter voltage (m_E). Fig. 3 shows the structure of the AC-voltage regulator. DC-voltage regulator controls the DC voltage across the DC capacitor of the STATCOM.

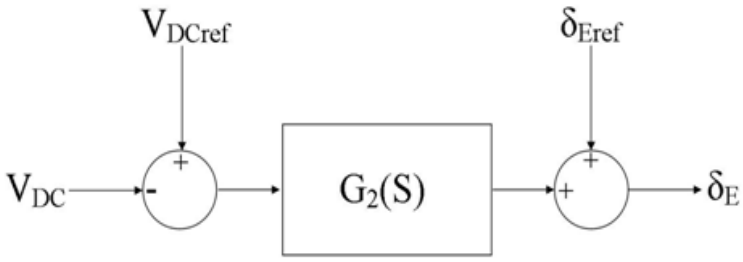

Fig. 4: DC-voltage regulator

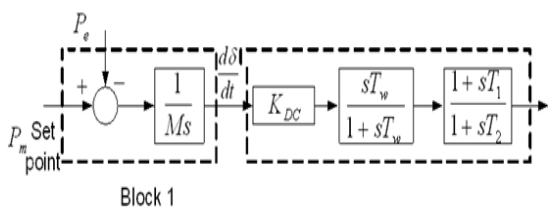

Fig. 5: The structure of damping controller

Table 1: Eigen-values of the closed-loop system without damping controller

-17.4561
+0.6151i±0.0205
-0.8834±0.6231

Table 2: Eigen-values of the closed-loop system with damping controller

-17.6132
-14.5865
-2.7532
-0.8511
-0.1021
-0.9251±0.9653i

Figure 4 shows the dynamic model of the DC-voltage regulator. The DC-voltage regulator functions by exchanging active power between the STATCOM and the power system. It is regulated by modulating the phase angle of the shunt converter voltage (δ_E).

Power system oscillations damping controller: A damping controller is provided to improve the damping of power system oscillations. This controller may be considered as a lead-lag compensator or the other methods (Yu, 1983; Eldamaty *et al*., 2005). However an electrical damping torque (ΔT_m) in phase with the speed deviation ($\Delta\omega$) is produced in order to improve the damping of power system oscillations. The transfer function block diagram of the damping controller is shown in Fig. 5.

System stabilization: For the nominal operating condition the eigenvalues of the system are obtained using state-space model of the system presented in (4) and these eigenvalues are shown in Table 1. It is clearly seen that the system is unstable and needs power system stabilizer (damping controller) for stability.

Damping controller design for stability: The damping controllers are designed to produce an electrical torque in phase with the speed deviation according to phase compensation technique. The two control parameters of the STATCOM (m_E and δ_E) can be modulated in order to produce the damping torque. In this study m_E is modulated to design damping controller. The speed deviation ω is considered as the input to the damping controller. The structure of damping controller is shown in Fig. 5. It consists of gain parameter (K_{DC}), signal washout parameter (Tw) and phase compensator block parameters (T1 and T2). The parameters of the damping controller are obtained using the phase compensation technique. The detailed step-by-step procedure for computing the parameters of the damping controller using phase compensation technique is presented in (Yu, 1983). Damping controller based m_B has been designed and obtained as (5):

$$\text{Damping controller} = \frac{387.211\ S\ (S+8.11)}{(S+0.1)\ (S+9.721)} \quad (5)$$

In the damping controller design the designing parameters have been considered as follow:

Wash-out block parameter T_w=10 and Damping ratio = 0.5

After applying this damping controller to system, the eigenvalues of the system with damping controller are obtained and shown in Table 2 and it is clearly seen that the system is stable.

Problem analysis: After system stabilization by applying the damping controller, The STATCOM AC-voltage and DC-voltage regulators are simultaneously designed based on the robust control technique. Since two controllers should be simultaneously designed, therefore the problem is a 2×2 MIMO problem and the design technique for MIMO systems should be considered. Since controller design for MIMO systems is a sophisticate procedure, so

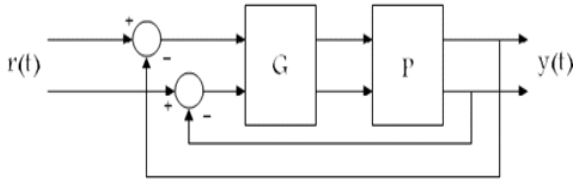

Fig. 6: The structure of MIMO control system (2×2)

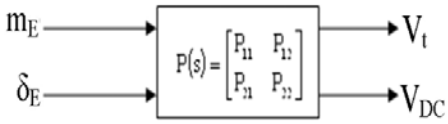

Fig. 7: Open-loop system for AC-voltage and DC-voltage control

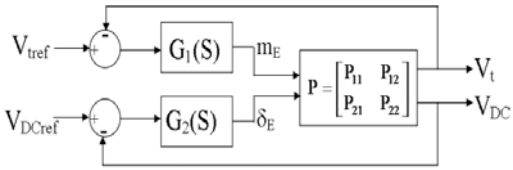

Fig. 8: Closed-loop system for AC-voltage and DC-voltage control containing compensators G_1 and G_2

in first the MIMO system is converted to equivalent MISO systems and then controllers are designed for these MISO systems. Using fixed point theory introduced in (Horowitz, 1982), a 2×2 MIMO system can be decentralized into 2 equivalent single-loops MISO systems (2 inputs and one output). Each MISO system design is based upon the specifications relating its output and all of its inputs. The basic MIMO compensation for a 2×2 MIMO system is shown in Fig. 6.

It consists of the uncertain plant matrix P(S) and the diagonal compensation matrix G(S). These matrices are defined as (6):

$$\begin{cases} P(s) = [P_{ij}](s) = \begin{bmatrix} P_{11} & P_{12} \\ P_{21} & P_{22} \end{bmatrix} \\ G(s) = diag\{G_i(s)\} = \begin{bmatrix} G_1 & 0 \\ 0 & G_2 \end{bmatrix} \end{cases} \tag{6}$$

Fixed point theory develops a mapping that permits the analysis and synthesis of a MIMO control system by a set of equivalent MISO control systems. For a 2×2 system, this mapping results in 2 equivalent systems, each with two inputs and one output. One input is designated as a desired input and the other as a disturbance input. The inverse of the plant matrix is represented by (7):

$$P(s)^{-1} = \begin{bmatrix} P_{11}^* & P_{12}^* \\ P_{21}^* & P_{22}^* \end{bmatrix} \tag{7}$$

Two effective plant transfer functions are formed as (8):

$$qij = \frac{1}{p*_{ij}} = \frac{\det. p}{adi. p_{ij}} \tag{8}$$

The Q matrix is then formed as (9):

$$Q = \begin{bmatrix} q_{11} & q_{12} \\ q_{21} & q_{22} \end{bmatrix} = \begin{bmatrix} \frac{1}{P*_{11}} & \frac{1}{P*_{12}} \\ \frac{1}{P*_{21}} & \frac{1}{P*_{22}} \end{bmatrix} \tag{9}$$

The matrix P^{-1} is partitioned to the follow form:

$$P^{-1} = [P*_{ij}] = \left[\frac{1}{q_{ij}}\right] = \Lambda + B \tag{10}$$

The system control ration (system transfer function) relating r to y is $T = [I+PG]^{-1}PGF$.

Pre multiplying of system control ration by [I+PG] yields: [I+PG] T = PGF

When P(S) is nonsingular, Pre-multiplying both sides of this equation by P^1 yields: $[P^{-1}+G]$ T = GF

Using (10), and with G diagonal, $[P^{-1}+G]$ T = GF can be rearranged as (11):

$$T = [\Lambda + G]^{-1}[GF - BT] \tag{11}$$

This equation is used to define the desired fixed point mapping where each of the 4 matrix elements on the right side of this equation can be interpreted as a MISO problem. Proof of the fact that design of each MISO system yields a satisfactory MIMO design is based on the fixed point theorem (Horowitz, 1982).

Based on the above discussions, in this study the STATCOM control problem characteristics are as follow:

- Controllers: AC-voltage and DC-voltage regulators
- Number of controllers: 2 controllers for STATCOM
- Plant matrix P(S) is a 2×2 matrix
- Diagonal compensation matrix G contains two compensators G_1 and G_2

Using dynamic state-space model of the SMIB power system presented in (4), the plant transfer function matrix P(S) is obtained with the related inputs and outputs which have been shown in Fig. 7. Where, the P(S) is uncertain plant transfer function of system and it is a 2×2 matrix.and G_1 and G_2 Using Fig. 7, the structure of the control loop can be shown as Fig. 8. Where P(S) is obtained using the state space model of the system presented in (4) at all operating conditions compensators are designed so that the variations of V_t and V_{DC} (system outputs) be within an acceptable range under all operating conditions.

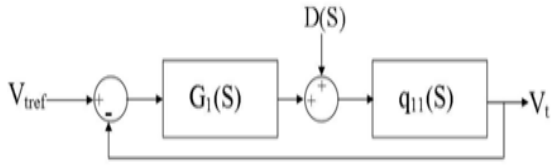

Fig. 9: The structure of closed-loop system for AC-voltage control

The System operating conditions have been defined in Appendix. According to these operating conditions and plant transfer function for any operating condition, the effective plant transfer functions defined in (9) (q_{11} and q_{22}) are obtained at any operating condition. Then, according to fixed point theory, AC-voltage regulator (G_1) is designed based on the effective plant transfer function q_{11} and DC-voltage regulator (G_2) is designed based on the effective plant transfer function q_{22}. In fact the MIMO problem is converted to two MISO problems. In the next part, the controller design process for these MISO systems is proposed using QFT method.

STATCOM controllers design using QFT: Quantitative Feedback Theory (QFT) is a unified theory that emphasizes to use of feedback for achieving the desired system performance tolerances despite plant uncertainty and plant disturbances. QFT quantitatively formulates these two factors as the following form:

- Sets $\tau_R = \{T_R\}$ of acceptable command or tracking input-output relations and sets $\tau_D = \{T_D\}$ of acceptable disturbance input-output relations
- Sets $\rho = \{P\}$ of possible plants

The objective is to guarantee that the control ratio (system transfer function) $T_R = Y/R$ is a member of τ_R and $T_D = Y/D$ is a member of τ_D for all P(S) in ρ. QFT is essentially a frequency-domain technique and in this study it is used for multiple input-single output (MISO) systems. It is possible to convert the MIMO system into its equivalent sets of MISO systems to which the QFT design technique is applied. The objective is to solve the MISO problems, i.e., to find compensation functions which guarantee that the performance tolerance of each MISO problem is satisfied for all P in ρ. The detailed step-by-step procedure to design controllers using QFT technique is given in (Dazzo and Houpis, 1988; Horowitz, 1982; Horowitz, 1979).

AC-voltage regulator design: Based on the descriptions in the section 6, the structure of control system for AC-voltage regulator is shown in Fig. 9. It can be clearly seen that the system is a MISO system and the compensator G_1 will be designed based on q_{11} (Horowitz, 1982).

In QFT-Based techniques introduced in (Dazzo and Houpis, 1988; Horowitz, 1982; Horowitz, 1979), the first step in the design process is to plot the plant uncertainties in Nichols diagram. This plot is known as system templates. The Templates of q_{11} are obtained by MATLAB software (2006) in some frequencies and shown in Fig. 10.

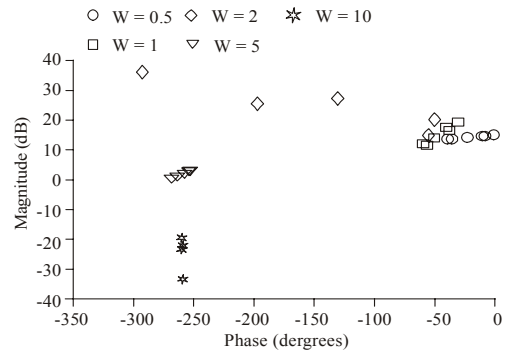

Fig. 10: Templates of effective plant transfer function q_{11}

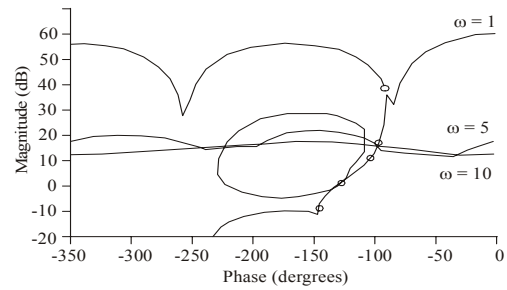

Fig. 11: Bounds and loop shaping for q_{11}

Compensator G_1 is designed so that the variation of output response (V_t) be within the acceptable range under the uncertainties of q_{11}. Since V_{tref} does not change in actual and simulation, therefore considering the tracking bounds is not necessary and consequently the tracking bounds are not considered, but for disturbance rejection purpose, the disturbance rejection bounds are considered to design G_1 compensator. Output response (generator terminals voltage) is acceptable if its magnitude is below the limits given by the disturbance rejection bounds. Based on the desired performance, the disturbance rejection bounds are obtained according to QFT method using QFT toolbox of MATLB software. Since in this case the tracking bounds have not been considered, so the disturbance rejection bounds ($B_D(j\omega i)$) are considered as composite bounds (B_O ($j\omega i$)). Also minimum damping ratios ξ for the dominant roots of the closed-loop system is considered as ξ = 1.2 and this amount on the Nichols chart establishes a region which must not be penetrated by the template of loop shaping (Lo) for all frequencies. The boundary of this region is referred to as U-contour. The U-contour and composite bound ($B_O(j\omega i)$) and an optimum loop shaping (L_{01}) based these bounds are shown in Fig. 11. Using L_{01} the compensator G_1 is obtained as (12):

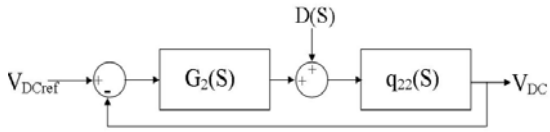

Fig. 12: The structure of closed-loop system for DC-voltage control

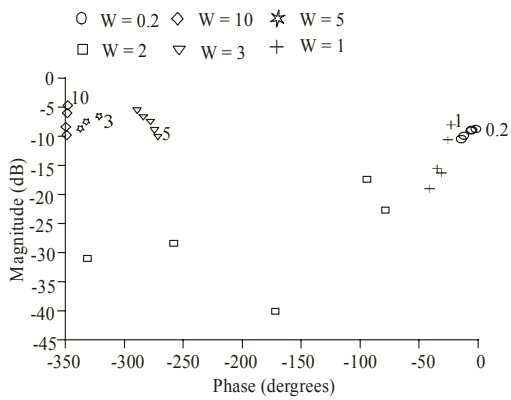

Fig. 13: Templates of effective plant transfer function q_{22}

$$G_1(s) = \frac{L_{02}(s)}{q_{22}(s)} = \frac{87.37(S^2 + 6.832S + 9.734)}{S(S + 20.561)(S^2 + 2S + 28.91)} \quad (12)$$

DC-voltage regulator design: The structure of control system for DC-voltage regulator is shown in Fig. 12. It is seen that the system is a MISO system and the compensator G_2 will be designed based on q_{22}.

The compensator G_2 is designed so that the variation of output response (V_{DC}) is within an acceptable range under all uncertainties of q_{22} and all operating conditions. Templates of q_{22} in some frequencies are shown in Fig. 13.

Similar to the former casee, since V_{DCref} does not change in actual system and simulation, therefore the tracking bounds are not considered for output and the disturbance rejection bounds are considered to design G_2 compensator. Outputresponse (DC-voltage of STATCOM) is acceptable if the magnitude of the output is below the limits given by the disturbance rejection bounds. Based on the desired performance, the disturbance rejection bounds are obtained based on QFT method using QFT toolbox of MATLB software. As mentioned before, since applying the input step to V_{DCref} is not actual, the tracking bounds are not considered and the disturbance rejections bounds (B_D (jωi)) are considered as composite bounds (B_O(jωi)). The U-contour and composite bound (B_O (jωi)) and an optimum loop shaping (L_{O2}) based on these bounds are shown in Fig. 14.

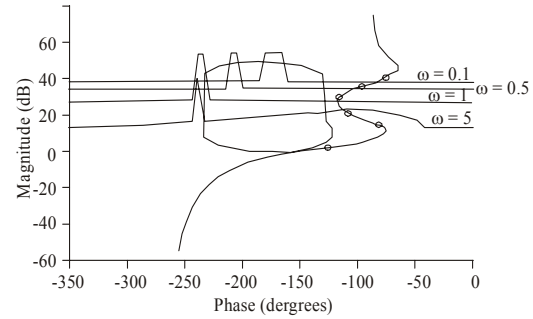

Fig. 14: Bounds and loop shaping for q_{22}

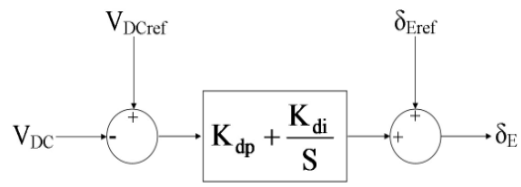

Fig. 15: PI type DC voltage regulator

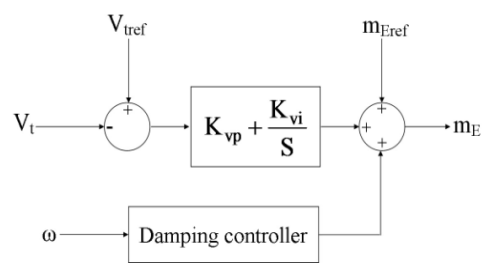

Fig. 16: PI type AC voltage regulator with damping controller

Using L_{O2} the compensator G_2 is obtained as (13) (the order has been reduced by model reduction technique).

$$G_2(s) = \frac{L_{02}(s)}{q_{22}(s)} = \frac{333.90(S + 3.23)(S + 2.012)}{S(S + 25.16)(S^2 + 108.943S + 2953)} \quad (13)$$

STATCOM controllers design using genetic algorithms: To show the effectiveness of QFT controllers, it is suitable to compare performance of QFT controllers with classical controllers. In classical case, PI type controller is considered for AC-voltage and DC-voltage regulators. Figure. 15 and 16 show the transfer function of the PI type DC and AC voltage regulators. The parameters of the AC-voltage regulator (K_{vp} and K_{vi}) and DC-voltage regulator (K_{dp} and K_{di}) are optimized and obtained using Genetic Algorithm (Randy and Sue, 2004) Optimum values of the proportional and integral gain setting of the AC voltage regulator are obtained as K_{vp} =

Table 3: Performance index following 5% step change in the reference mechanical torque (ΔTm)

	Performance index	
	Genetic algorithms	QFT
Operating condition 1	0.0431	0.0425
Operating condition 2	0.0492	0.0483
Operating condition 3	0.0574	0.0521
Operating condition 4	0.0599	0.0568
Operating condition 5	0.0612	0.0593
Operating condition 6	0.0506	0.0479

4.48 and K_{vi} = 4.98. When the parameter of AC-voltage regulator are set at their optimum values, the parameters of DC-voltage regulator are now optimized and obtained as K_{dp} = 0.6719 and K_{di} = 0.412 (Taher *et al.*, 2008a).

SIMULATION RESULTS

In this section QFT and optimal PI controllers are applied to system and compared. The classical method to compare their responses is to show responses following step change at inputs. Since showing many figures is not favorable, so a performance index can be considered for more comparison purposes. Here, the performance index is defined as follow:

$$\text{Performance index} = \int_o^t |\Delta\omega| dt + \int_o^t |\Delta V_{DC}| dt + \int_o^t |\Delta V_t|$$

In fact the performance index is the total area under the curves (output responses) and this performance index is a suitable benchmark to compare performance of robust controllers and optimal PI controllers. The parameter "t" in performance index is the simulation time and considered form zero to settling time of response. It is clear that the controller with lower performance index has better performance than the other controllers. The performance index has been calculated following 5% step change in the reference mechanical torque (ΔTm) in several operating conditions (The operating conditions have been given in Appendix). The result is given in Table 3. It is clear to see that QFT controllers have better performance than optimal PI controllers at all operating conditions. QFT controllers have lower performance index in comparison with optimal PI controllers and therefore the QFT controllers can mitigate power system oscillations successfully.

Although the table result is enough to compare robust methods, it is useful to show the responses. Figure 17 shows the dynamic responses for a 10% step change in the reference mechanical torque (ΔTm) with QFT and optimal PI controllers. This figure shows that QFT controllers have better performance in voltage control and damping of power system oscillations in comparison with optimal PI controllers. With QFT controllers the DC-voltage and AC-voltage are driven back to zero following step change in the reference mechanical torque (ΔTm).

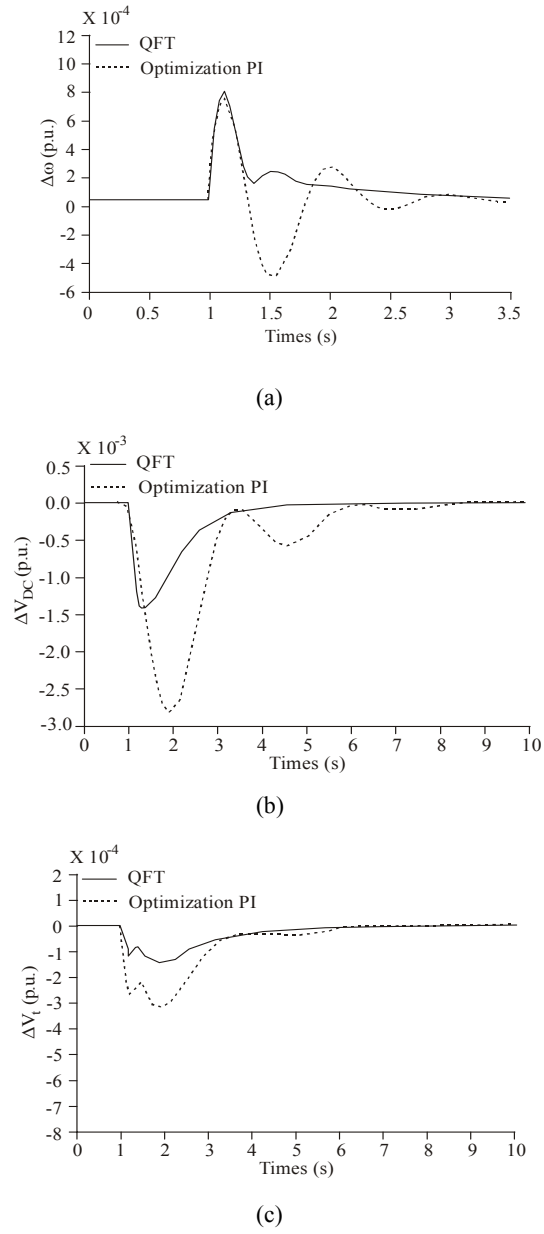

Fig. 17: Dynamic responses at nominal load (operating condition 1), following 10% step change in the reference mechanical torque (ΔT_m); (a): Dynamic response Δω (b): Dynamic response ΔV_{DC} (c): Dynamic response ΔV_t

CONCLUSION

In this study a robust decentralized STATCOM controller design was proposed. QFT method was

considered and applied to design controllers. This design strategy includes enough flexibility to set the desired level of stability and performance and consider the practical constraints by introducing appropriate uncertainties. The proposed method was applied to a typical SIMB power system installed with STATCOM with system parametric uncertainties and various load conditions. The simulation results demonstrated that the designed controllers were able to guarantee the robust stability and robust performance under a wide range of parametric uncertainties and load conditions. Also, simulation results showed that this method is robust to the change of system parameter.s the proposed method has an excellent capability in damping power system oscillations and enhancing power system stability

Appendix:

The nominal parameters and operating conditions of the system are listed in Table 4.

In this research, the system uncertainties are defined by 40% load change from their typical values (contain active and reactive powers). The uncertainty areas for active and reactive powers are defined as follow:

$0.7 \le P \le 1.125$ and $0.1 \le Q \le 0.3$

Using defined uncertainties, six operating conditions are defined and the parameters of these operating conditions are shown in Table 5, where, the operating condition 1 is the nominal operating condition.

SYMBOLS AND ABBREVIATIONS

STATCOM	: Static Compensator
SVC	: Static Var Compensator
PI controller	: Proportional-Integral controllers
QFT method	: Quantitative Feedback Theory method
SMIB power system	: Single-Machine Infinite Bus power system
FACTS: Flexible devices	: AC Transmission Systems devices
SISO system	: Single Input – Single Output system
MISO system	: Multi Input – Single Output system
MIMO system	: Multi input – Multi Output system
PWM	: Pulse Width Modulation

System control ration from input to output: System transfer function from input to output:

ω	: Synchronous speed of the system
δ	: Torque angle
P_m	: Mechanical input power
P_e	: Electrical output power
M	: Equivalent inertia of the system
D	: Mechanical damping coefficient
E_q'	: Voltage behind the transient reactance
E_q	: Internal voltage of armature (synchronous generator)
E_{fd}	: Internal voltage of armature (synchronous generator)
T'_{do}	: Open circuit-transient time constant of d axis
K_a	: Gain of voltage regulator
T_a	: Time constant of voltage regulator
V_{ref}	: Reference voltage of voltage regulator
V_t	: Generator terminal voltage
V_{dc}	: DC-link voltage
C_{dc}	: DC-link capacitor
m_E	: Pulse width modulation index of inverter
δ_E	: Phase angle of the shunt inverter voltage
I_{ed}	: d-axis current of STATCOM
I_{eq}	: q-axis current of STATCOM
K_{ij}	: System constant coefficients
T_m	: Mechanical input torque
T_e	: Electrical output torque
Δ	: Deviation from nominal value
ω_0	: Initial value of speed
δ_0	: Initial value of torque angle

$$\dot{E}_q^t = \frac{d}{dt}E_q^t, \quad \dot{\delta} = \frac{d}{dt}\delta, \quad \dot{\omega} = \frac{d}{dt}\omega$$

$$\dot{E}_{fd} = \frac{d}{dt}E_{fd}, \quad \dot{V}_{dc} = \frac{d}{dt}V_{dc}$$

ACKNOWLEDGMENT

The authors gratefully acknowledge the financial and other support of this research, provided by Islamic Azad University, Islamshahr Branch, Tehran, Iran.

Table 4: Nominal system parameters

Generator	M = 8 Mj/MVA	T'_{do} = 5.044 s	X_d = 1 p.u.
	X = 0.6 p.u. $_q$	X´d = 0.3 p.u.	D = 0
Excitation system		K_a = 10	T_a = 0.05 s
Transformers		X_{te} = 0.1 p.u.	X_{SDT} = 0.1 p.u.
Transmission lines		X_{T1} = 1 p.u.	X_{T2} = 1.25 p.u.
Operating condition	V_t = 1.03 p.u.	P = 1 p.u.	Q = 0.2 p.u.
DC link parameters		V_{DC} = 2 p.u.	C_{DC} = 3 p.u.
STATCOM parameters		Δ_e = 27.19°	M_e = 1.0962

Table 5: System operating conditions

Operating condition 1	P = 1.00 p.u.	Q = 0.20 p.u.	V_t = 1.03 p.u.
Operating condition 2	P = 0.90 p.u.	Q = 0.17 p.u.	V_t = 1.03 p.u.
Operating condition 3	P = 1.10 p.u.	Q = 0.25 p.u.	V_t = 1.03 p.u.
Operating condition 4	P = 1.15 p.u.	Q = 0.30 p.u.	V_t = 1.03 p.u.
Operating condition 5	P = 1.20 p.u.	Q = 0.35 p.u.	V_t = 1.03 p.u.
Operating condition 6	P = 0.70 p.u.	Q = 0.10 p.u.	V_t = 1.03 p.u.

REFERENCES

Ammari, S., Y. Besanger, N. Hadjsaid and D. Ggeorges, 2000. Robust Solutions for the Interaction Phenomena between Dynamic Loads and FACTS Controllers, Proc. IEEE PES Summer Meeting, pp: 401-406.

Dazzo, J.J. and C.H. Houpis, 1988. Linear Control System Analysis and Design Conventional and Modern, McGraw Hill..

Edwards, C.W., K.E. Mattern, E.J. Stacey, P.R. Nannery and J. Gubernick, 1988. Advanced Static VAR Generator Employing GTO Thyristors. IEEE Trans. Power Deliver. 3(4): 1622-1627.

Eldamaty, A., S.O. Faried and S. Aboreshaid, 2005. Damping Power System Oscillation Using a Fuzzy Logic Based Unified Power Flow Controller, IEEE CCECE/CCGEI, pp: 1950-1953.

Farasangi, M.M., Y.H. Song and Y.Z. Sun, 2000. Supplementary Control Design of SVC and STATCOM Using H∞, Optimal Robust Control, proc. Int. Conf. on Electric Utility Deregulation 2000, City University, London, pp: 355-360.

Hingorani, N.G. and L. Gyugyi, 2000. Understanding FACTS, IEEE Press, New York.

Horowitz, I.M., 1979. Quantitative synthesis of the uncertain multiple input-output feed back systems. Int. J. Control, 30: 81-106.

Horowitz, I., 1982. Quantitative Feed back Theory, IEEE Proc. D., 129(6): 215-226.

Li, C., O. Jiang, Z. Wang and D. Retzmann, 1998. Design of a Rule Based Controller for STATCOM, Proc. 24th Annual Conf. of IEEE Ind. Electronic Society. IE Con 98, pp: 467-472.

MATLAB Software, 2006. Robust Control Toolbox. QFT Tool Box, Math Works, Inc.

Mori, S., K. Matsuno, M. Takeda and M. Seto, 1993. Development of a Large Static VAR Generator Using Self-Commutated Inverter for Improving Power System Stability. IEEE Trans. Power Syst., 8(1): 371-377.

Randy, L.H.and E.H. Sue,2004. Practical Genetic Algorithms. 2nd Edn., John Wiley & Sons.

Schauder, C., M. Gernhardt, E. Stacey, T. Lemak, L. Gyugyi, T.W. Cease and A. Edris, 1994. Development of a +/-100 MVAR Static Condenser for Voltage Control of Transmission Systems, IEEE Power Engineering Society, Summer Meeting, pp: 479-6-1-8.

Taher, S.A., R. Hemati and A. Abdolalipour, 2009. UPFC Controller Design Using QFT Method in Electric Power Systems, International IEEE Conference, Saint Petersburg, Russia.

Taher, S.A., R. Hematti and M. Nemati, 2008a. Comparison of different control strategies in ga-based optimized UPFC controller in electric power systems. Am. J. Eng. Appl. Sci., 1(1): 46-53.

Taher, S.A., S. Akbari, A. Abdoalipour and R. Hematti, 2008b. Design of robust UPFC controllers using h_∞ control theory in electric power system. Am. J. Appl. Sci., 5(8): 980-989.

Taher, S.A., S. Akbari and R. Hematti, 2008c. Design of robust decentralized control for UPFC controllers based on structured singular value. Am. J. Appl. Sci., 5(10): 1269-1280.

Wang, H.F., 1999a. Damping function of unified power flow controller. IEE Proc. Gen. Trans. Dist., 146(1): 129-140.

Wang, H.F.,1999b. Phillips-Heffronmodelof power systems installed with stat com and applications. IEE Proc. Gen. Trans. Dis. 146(5).

Wang, H.F. and F. Li, 2000a. Design of STATCOM Multivariable Sampled Regulator, International Conference on Electric Utility Deregulation and Power Technology, City University, London.

Wang, H. and F. Li, 2000b. Multivariable Sampled Regulators for the Coordinated Control of STATCOM AC and DC Voltage. IEE Proc. Gen., Trans. Dis., 147(2): 93-98.

Yu, Y.N., 1983. Electric Power System Dynamics, Academic Press, Inc., London.